Journal of Physics: Conference Series **2793** (2024) 012008 doi:10.1088/1742-6596/2793/1/012008

Predicted yield and detectability of GW events from the IllustrisTNG simulations

Luchang Niu[1,*], **Tiangang Zhang**[2], **Kun Zhang**[2] **and Yiting Li** [3]

[1]Department of Physics and Astronomy, University of Rochester, 14627, USA
[2]School of Physics, Beihang University, Beijing, 102600, China
[3]University of Michigan, Ann Arbor, department of astronomy, USA 48109

* Corresponding author's email: niuluchang12345@126.com

Abstract. The forthcoming generation of space-based gravitational wave (GW) observatories promises robust capabilities for multi-bandwidth measurements, particularly for the study of supermassive black holes (SMBHs). In this research, we employ the IllustrisTNG simulation to investigate GW signals originating from SMBHs. Our approach involves extracting the merger history of black holes (BHs) from the simulation data and utilizing a phenomenological waveform model to calculate the GW strains, signal-to-noise ratios and event rates. Notably, detectors like LISA, Taiji, and Tianqin demonstrate the potential to detect SMBHs with masses exceeding approximately $10^6 M_\odot$, and exhibit the capability to detect one merger in the Merger-Ringdown phase and one merger in the Inspiral phase annually, at redshifts reaching up to $z\sim6$.

1. Introduction

Gravitational waves (GWs), first envisioned by Albert Einstein in his 1916 general theory of relativity, are spacetime ripples generated by massive accelerating objects[1], which can be detected by GW detectors. While ground-based detectors cannot detect sub-1 Hz gravitational waves necessary for studying massive black holes (MBHs) and supermassive black holes (SMBHs) due to terrestrial gravity gradient noise. However, these lower-frequency waves are observable with space-based instruments

Space-based interferometers, such as the Laser Interferometer Space Antenna[2], operate within a frequency range of 10^{-4} to 10^{-1} Hz. This range enables the detection of mergers involving massive black holes (MBHs) in the mass spectrum of approximately 10^4 to $10^7 M_\odot$during the reionization epoch[3]. Research groups employ diverse methods, including analytical calculations[4] and cosmological simulations[5], to estimate black hole (BH) merger rates and predict gravitational wave (GW) signals.

2. Methods

2.1. Cosmological simulations

The IllustrisTNG project[6] comprises a collection of advanced cosmological simulations that model the formation of the universe. These simulations encompass a significant portion of a simulated universe, starting from the early stages after the Big Bang and progressing to the present day. They incorporate various physical processes that influence galaxy formation. There are three volumes in the original

IllustrisTNG project with a total of 18 simulations, each demonstrating variations in physical size, mass resolution, etc. [6]. The side length of simulation box is 35000.0, 75000.0, 205000.0 [ckpc/h] for TNG50, TNG100 and TNG300 respectively. TNG100 are used in this study. The simulations use the cosmological parameters of Planck2015 (i.e. total matter density $\Omega_m = 0.3089$, dark energy density $\Omega_\Lambda = 0.6911$, baryonic matter density $\Omega_b = 0.0486$, hubble constant 'little h' $h_0 = 0.6774$ [100km/s/Mpc]). The number of dark matter particles of TNG100 is 6028568000 with no gas tracer particles.

2.1.1. *Black Hole Mergers.* Merging binary black hole (BBH) systems are characterized by intrinsic parameters: individual BH masses (m_1 and m_2), spin angular momenta ($\overrightarrow{S_1}$ and $\overrightarrow{S_2}$), leading to dimensionless spin magnitudes $\chi_{1,2} \equiv c\left|\overrightarrow{S_{1,2}}\right|/\left(Gm_{1,2}^2\right)$, and the gravitational wave frequency f. Additionally, luminosity distance computed from redshift and orientation angles (ψ, ι, α, δ) are needed. The gravitational waveform produced by a binary black hole (BBH) merger depends on the system's mass ratio, spin, and distance.

The BH merger process comprises three phases: the inspiral phase, the merger phase and the ringdown phase. The inspiral phase is driven by gravitational radiation damping, causes a gradual orbital decay. It ends when the black hole separation approaches the innermost stable circular orbit (ISCO) with $r_{isco} > 6GM/c^2$, where $M = m_1 + m_2$. During this phase, binary dynamics and gravitational waveforms are described using post-Newtonian expansions[7]. The merger phase begins when the binary reaches its highest orbital frequency (ISCO or merger frequency f_{isco}), or when the radiation-reaction timescale matches the orbital period. The separation decreases rapidly, transitioning from inspiral to plunge, occurring for orbits more tightly bound than the ISCO[8]. In the ringdown phase, the system settles into a Kerr black hole state, emitting gravitational waves due to deviations from its final axisymmetric form. This phase's dynamics are accurately described as oscillations of the final black hole's quasinormal modes, using perturbation theory on the Kerr spacetime background[9].

2.1.2. Treatment of the Inspiral and Merger Phases for the BBHs from the Cosmological Simulations. In cosmological simulations, the formation of a binary black hole (BBH) occurs when two black holes become gravitationally bound. To model the inspiral and merger phases, we adopt a similar approach as employed in other studies[5]. We initiate the inspiral phase when the BBH enters the spatial resolution range, and the timescale for inspiral is calculated as follows.

In the Newtonian limit, the orbital radius r and orbital angular velocity Ω are interconnected through the Keplerian relationship (Unless specified otherwise, we use the geometric system of units in which $G = c = 1$): $\frac{M}{r} \equiv \frac{1}{\tilde{r}} \equiv (M\Omega)^{2/3} \equiv \widetilde{\Omega}^{2/3}$. Here, $\tilde{r}$ and $\widetilde{\Omega}$ represent the dimensionless radius of the orbit and the dimensionless orbital angular velocity, respectively. The gravitational wave frequency for a specific harmonic mode m is expressed as $f_m = \frac{m}{2\pi M\widetilde{\Omega}}$. Our analysis focuses only on the dominant $m = 2$ mode, for which the associated frequency is given by $f_2 = \frac{\Omega}{\pi}$.

In the limit where $m_2 \gg m_1$, the total duration of the inspiral phase until the innermost stable circular orbit (ISCO) is attained[10], denoted as T_{insp}, is given by:

$$T_{\rm insp} = \frac{5}{256}\frac{1}{\eta}\frac{M}{\widetilde{\Omega}^{8/3}}\tau = 1.41\times10^6\ \sec\left(\frac{f_2}{10\ \rm mHz}\right)^{-8/3}\left(\frac{10}{m_1}\right)\left(\frac{10^6 M_\odot}{M}\right)^{2/3}\tau$$
$$= 0.141\ \sec\left(\frac{f_2}{100\ \rm Hz}\right)^{-8/3}\left(\frac{10M_\odot}{m_1}\right)\left(\frac{100M_\odot}{M}\right)^{2/3} \quad (1)$$

Here, $\eta = m_1 m_2/M^2$ represents the symmetric mass ratio, with M being the total mass. Additionally, τ denotes the relativistic correction to T_{insp}, a function dependent on the orbital radius r/r_{isco} and the black hole spin parameter[11]. The parameter r/r_{isco} can be determined as the ratio of f_2 and f_{isco}

concurrently: $\frac{r}{r_{isco}} = (f/f_{isco})^{-2/3}$. The ISCO is located at $\tilde{r}_{isco}$, where the total energy $E(\tilde{r})$ of the object is minimized, or equivalently, where the time derivative of Ω becomes infinite. The value of $\tilde{r}_{isco}$ can be determined as the root of the quartic equation $\tilde{r}^2 - 6\tilde{r} + 8\chi\tilde{r}^{1/2} - 3\chi^2 = 0$. This value lies between 1 (when χ =1) and 6 (when χ =0). In our analysis, where the BH spin is assumed to be 0, the frequency at the ISCO is calculated as:

$$f_{2,\mathrm{isco}} = \frac{\Omega}{\pi} = \frac{\widetilde{\Omega}_{isco}}{\pi M} = \left(\frac{1}{\tilde{r}_{isco}}\right)^{3/2} / \pi M = \frac{\tilde{r}_{isco}{}^{-3/2}}{M\pi} = \frac{6^{-3/2}}{M\pi} \quad (2)$$

For each binary black hole (BBH) obtained from the cosmological simulations, we incorporate the timescale T_{insp} to represent the inspiral phase. Beyond this period, we assume that the BBH coalesces, transitioning into the merger phase.

2.2. Gravitational wave calculations

In our calculations of gravitational waves emanating from binary black holes (BBHs), we utilize the notation Ξ to represent the physical parameters of a BH binary, where $\Xi \in (M, \eta, \chi_1, \chi_2)$. Here, M is the total mass of the BBH, η signifies the mass ratio, and χ_1 and χ_2 are the spin parameters of the BHs. Here, the spin parameters χ_i fall within the range of $[-1,1]$.

We utilize the "PhenomD" model[12] in our study to compute GW amplitudes in the Fourier domain. The "PhenomD" model is a hybrid waveform model that combines an analytical effective-one-body (EOB) model with numerical relativity (NR) simulation data. Within this model, the Inspiral phase is described using the uncalibrated EOB model from the minimum frequency up to the transition frequency f_{isco}. Beyond this frequency, the model switches to NR simulations to accurately model the Merger-Ringdown waveforms spins[13]. The amplitude of the gravitational wave signal from such a system also depends on the luminosity distance[14].

The sensitivity of a GW detector is often described by the root power spectral density (PSD), $\sqrt{S(f)}$. In contrast, the amplitude of a GW source can be expressed by the characteristic strain. The square root PSD that describes the strain noise[15] is given by:

$$\sqrt{S_{\mathrm{n}}(f)} = h_{\mathrm{n}}(f) f^{-\frac{1}{2}} \quad (3)$$

Where the detector noise curve $S_n(f)$, may be acquired through either analytical fitting procedures or interpolation techniques applied to the sensitivity data. For this study, we select five space-borne interferometers Tianqin, Taiji, LISA, BBO, and DECIGO. In table 1, we list the GW detectors considered in this study, and summarize the analytical approximations of the PSD for each detector. For LISA, Taiji and Tianqin, we adopt the analytical fits[6,34]. The analytical approximations of the BBO and DECIGO noise curves are given by [17].

3. Results

3.1. Gravitational wave characteristic strain from black hole mergers

When a GW passes a detector, it imparts a fractional alteration in the detector's arm lengths. This alteration is captured and documented as a dimensionless strain with respect to time, given by $\mathrm{h(t)} = \frac{\triangle \mathrm{L(t)}}{\mathrm{L}}$. The characteristic strain is designed to incorporate the effect of integrating an inspiralling signal[15], whose amplitude is given by:

$$h_{\mathrm{c}}(f) = 4f^2 \left|\tilde{h}(f)\right|^2 \quad (4)$$

The symbol f represents the rest-frame frequency of the source, and $\tilde{h}(f)$ corresponds to the Fourier transform of the strain signal, which can be expressed as $\tilde{h}(f) = \mathcal{F}\{h(t)\}(f) = \int_{-\infty}^{\infty} h(t) e^{-2\pi i f t}$. Likewise, the characteristic noise strain pertaining to GW detectors can be calculated through a rearrangement of equation (3) where the term $S_{\mathrm{n}}(f)$ signifies the analytical approximation of the noise spectral densities, as itemized in table 1.

We adhere to a method[5] to compute $h_c(f)$ and $h_n(f)$ from our simulation data, which involves the following steps:

- Extract the merger tree of the simulation and determine the intrinsic parameters of each merging BBH pair at the moment of "merger" at a specific redshift (i.e., the merger redshift)..
- Segregate the coalescence process into the inspiral and merger-ringdown phases, in accordance with the method in section 2.1.2. The inspiral phase starts when the distance between the BBH pair falls below the spatial resolution threshold and continues for a duration of $T_{\rm insp}$ as defined in equation (1). Subsequently, the pair coalesces and enters the merger-ringdown phase.
- Utilize equation (2)) to compute the frequency at the moment of merger (the merger frequency $f_{\rm isco}$). Convert this frequency to the observed frequency $f_{\rm obs}$, via the relation $f_{\rm obs} = f_{\rm isco}/(1+z)$.
- Calculate the frequency-domain amplitudes of the GW signals $\left|\tilde{h}(f_{\rm obs})\right|$ with the "PhenomD" model, for all BH coalescence events in TNG100. This calculation assumes no BH spin.
- Use equation (4) to compute the characteristic strain amplitude at the observed merger frequency $h_c(f_{\rm obs})$.
- Use equation (5) to calculate the characteristic noise amplitude at the observed merger frequency $h_n(f_{\rm obs})$ of each GW detector.
- Utilize the "PhenomD" model to compute the theoretical projections of $h_c(f)$ for equal-mass, non-spinning BBH systems across a mass range spanning from $M_1 = M_2 = 10^4 M_\odot$ to $M_1 = M_2 = 10^{10} M_\odot$), at various redshifts, ranging from $z \approx 15$ to $z \approx 10^{-3}$.

Table 1. Parameters description of the corner plot.

Detector	Arm length (km)	Frequency (Hz)	$S_n(f)$
LISA	5×10^6	$3\times10^{-5}-1$	$\frac{10}{3L^2}\left(P_{dp}+2\left(1+cos^2\left(\frac{f}{f_*}\right)\frac{P_{acc}}{(2\pi f)^4}\right)\right)\left(1+0.6\left(\frac{f}{f_*}\right)^2\right)$
BBO	5×10^4	$10^{-3}-10$	$2\times10^{-49}f^2+4.58\times10^{-49}+1.26\times10^{-52}f^{-4}$
TIANQIN	$\sqrt{3}\times10^5$	$10^{-4}-1$	$\frac{10}{3L^2}\left[10^{-24}+\frac{4\times10^{-30}}{(2\pi f)^4}\left(1+\frac{10^{-4}Hz}{f}\right)\right]\times\left[1+0.6\left(\frac{f}{f_*}\right)^2\right]$
TAIJI	3×10^6	$10^{-4}-1$	$\frac{10}{3L^2}\left(P_{dp}+2\left(1+cos^2\left(\frac{f}{f_*}\right)\frac{P_{acc}}{(2\pi f)^4}\right)\right)\left(1+0.6\left(\frac{f}{f_*}\right)^2\right)$
DECIGO	10^3	$0.1-10$	$7.05\times10^{-48}[1+(f/7.36)^2]+4.8\times10^{-51}f^{-4}\frac{1}{1+(f/7.36)^2}+5.33\times10^{-52}f^{-4}$

[A] THE APPROXIMATED ANALYTICAL NOISE SPECTRAL DENSITY IN EITHER $S_N(f)$ OR $S_N(x)$, WHERE x IS DIMENSIONLESS FREQUENCY $x = f/f_0$. $f_* = \frac{c}{2\pi L}$. FOR LISA, $P_{dp} = (15\times10^{-12}m)^2\left(1+\left(\frac{2mHz}{f}\right)^4\right)Hz^{-1}$, $P_{acc} = (3\times10^{-15}ms^{-2})^2\left(1+\left(\frac{0.4mHz}{f}\right)^2\right)\left(1+\left(\frac{f}{8mHz}\right)^4\right)Hz^{-1}$. FOR TAIJI, $P_{dp} = (8\times10^{-12}m)^2\left(1+\left(\frac{2mHz}{f}\right)^4\right)Hz^{-1}$, S_{acc} IS SAME AS LISA.

Figure 1 displays the resultant GW characteristic strain amplitudes $h_c(f_{\rm obs})$, for all SMBH mergers at various redshifts in TNG100. These are compared with theoretical forecasts for equal-mass mergers at different redshifts. Additionally, sensitivity curves for GW detectors, namely Tianqin, LISA, Taiji, DECIGO, and BBO, are featured for reference. It's important to note that figure 1 only presents the $h_c(f_{\rm obs})$ values corresponding to the Merger-Ringdown phase for illustrative purposes.

Figure 1 shows a trend that the characteristic strain amplitude increases as the masses of the BH mergers increase, with decreased observed frequency. For these massive BH mergers of $\gtrsim 10^6 - 10^9\, M_\odot$, BBO and DECIGO can detect part of BH mergers of $10^6\, M_\odot$ at very low redshift dowm to $z \sim 1$, while LISA can detect mergers of $\backsim 10^6 - 10^{7.5}\, M_\odot$ in the redshift range $z \sim 7 - 10^{-3}$, but for more massive mergers of $\geq 10^8\, M_\odot$ and above, they move out of LISA's frequency range. For Tianqin and Taiji, they have a similar sensitivity curves as LISA but with a higher cut-off frequency which makes them detect

less massive BH mergers than LISA especially these BHs of $\gtrsim 10^7 - 10^8\, M_\odot$, but they can still detect mergers in the same range of redshift as LISA. The gravitational wave signals produced by the SMBH mergers shown in figure 1 closely agree with the results of other study[5].

3.2. Detectability of black hole mergers

A GW detector generates an output signal that combines noise, characterized by the noise PSD $S_{\rm n}(f)$, and a potential GW signal: $s(t) = n(t) + h(t)$. The separation of contributions from the signal and the noise can be accomplished through the convolution of the filter function associated with the Wiener filter with the detector's output[15].

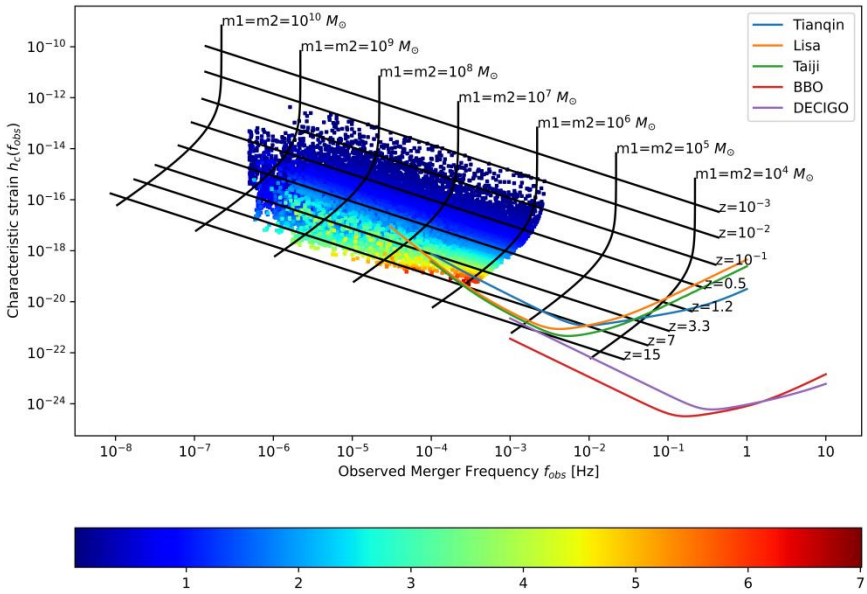

Figure 1. Colored data points represent BBH merger events in TNG100. These points are color-coded based on the redshift at the time of merger. Additionally, sensitivity curves for space-based gravitational wave detectors are displayed. Alongside them, black gridlines depict theoretical predictions for $h_{\rm c}$ originating from equal-mass, non-spinning BBH mergers. Data points positioned above a detector's sensitivity curve may be detectable by that particular detector, while those below the curve represent merger events that cannot be resolved by the detector.

we employ the matched-filtering methodology and the root-mean-square value for the SNR $\rho_{\rm rms}$ can be expressed as: $\rho^2_{\rm rms} = 4\int_0^\infty \frac{|\tilde{h}(f)|^2}{S_{\rm n}(f)} df$, where $\tilde{h}(f) = \int_{-\infty}^{\infty} e^{2\pi i f t} h(t)\, dt$ is the Fourier transform of the dimensionless strain $h(t)$ generated from the ``PhenomD" model.In the case of an inspiraling source, equation above no longer remains applicable. The precise definition of the characteristic strain $h_{\rm c}$, is derived directly from the definition of SNR as $\rho_{\rm rms} = \sqrt{\int \left(\frac{h_{c,m}(f_m)}{h_{\rm n}(f_m)}\right)^2 d\ln(f_m)}$ [18]. In the Merger-Ringdown phase, we establish the upper integration limit as infinity and the lower limit $f_{\rm isco}$ as expressed in Equation (2). The square of the SNR for the Merger-Ringdown phase can be precisely expressed as:$\rho^2 = 4\int_{f_{\rm isco}}^{\infty} \frac{|\tilde{h}(f)|^2}{S_{\rm n}(f_{\rm obs})} df_{\rm obs}$.

3.3. Event rate of black hole mergers

The count of detectable sources surpassing the detection threshold $SNR = 10$ within a redshift range from z to $z + dz$ is defined as $\bar{N}(z,\mathrm{SNR} \geq 10)/\triangle z\mathrm{V_c} \sim d^2\bar{n}(z,\mathrm{SNR} \geq 10)/dz d\mathrm{V_c}$, where $\mathrm{V_c}$ represents the co-moving volume. The estimated event rate of detected GW sources per observed time, considering the integration across all redshifts[19], is provided by:

$$\frac{d\bar{N}}{dt_{\text{obs}}} = \int_0^{\infty} \frac{d^2\bar{n}(z, SNR \geq 10)}{dz} \frac{dz}{dt} \frac{dV_c}{dz} \frac{dz}{(1+z)} \tag{5}$$

To assess the count of resolvable events originating from inspiral and merger-ringdown sources within the binary black hole (BBH) simulations, we designate signals with SNR ≥ 10 whose observed merger frequency falls within the frequency range of the target detector (as specified in table 1) as detectable. Because TNG100 lack the resolution required to determine the spin of each individual BH, we employ $\chi_1 = 0$ and $\chi_2 = 0$ for the merging BH pairs. Recent research[5] suggests that spin contributions to the event rate across all phases are negligible.

Table 2 provides an overview of the approximated counts of detectable signals and the corresponding event rates originating from inspiral, merger-ringdown, and complete inspiral-merger-ringdown sources within TNG100, considering various GW detectors. For the super massive black holes ($M_{\odot} \geq 10^6$), only very small part of the BBH events in TNG100 fall inside of the frequency range of the BBO and DECIGO, so they will be able to resolve less BH mergers than other detectors.

Table 2. Estimates of resolvable signals (SNR ≥ 10) and event rates of inspiral, merger-ringdown (Mrd), and full inspiral-merger-ringdown (full-IMR) sources from IllustrisTNG for various gravitational wave detectors.

Detector	Number of Resolvable Inspiral Signals	Number of Resolvable Mrd Signals	Detection Rates of Inspiral Signals (yr^{-1})	Detection Rates of Mrd Signals (yr^{-1})
Tianqin	6757	6773	1.00	1.02
Taiji	6796	6796	1.03	1.03
LISA	9167	9248	1.18	1.19
DECIGO	593	593	0.01	0.01
BBO	593	593	0.01	0.01

[a] Numbers of mergers events is 18282.

The number of resolvavle signals and event rate of BBO and DECIGO are same because their sensitivity curves are very similiar and do not reach to the area of bh mergers(see figure 1). Each of Tianqin, Taiji, LISA will be able detect about 1 merger event of Merger-Ringdown phase and Inspiral phase per year respectively while BBO and DECIGO will not be able to detect almost any signals of either phase per year.

3.4. Parameters distribution of detectable events

The distribution of different parameters of SMBH merger events is an important indicator of the environments in which they grow, the star formation rate (SFR). They are very useful when study the origin and formation of these super massive black holes.

Figure 2 shows the corner plot super massive bh mergers in IllustrisTNG. The hists in green are the parameters (Table 3) distributions of resolvable mergers events while the hists in blue are distributions of irresolvable merger events. The red contours describe the relationship between these parameters related resolvable merger events.

We can see from figure 2 that the distribution of Rho(Local gas density in the vicinity of the blackhole) is the superposition of two normal distribution with two differnet peaks. However the BH mergers resolvable by LISA are only distributed by one of the normal distribution. Almost all the BHs of another normal distribution are irresolvable. Similarity, Mdot(The mass accretion rate onto the black hole, instantaneous) has two peaks as well but GW detectors can only detect BHs gathering around one of the peaks. In Rho-Mdot plot, there are clearly three peaks but only BHs around one of the peaks can be detected by LISA. In fact, we have a relation between Cs and Rho: $\dot{M_{BH}} = (4\pi G^2 M_{BH}^2 \rho)/(c_s^2 + v_{rel}^2)^{\frac{3}{2}}$, where ρ and c_s are the Local gas density and Local gas sound-speed in the vicinity of the black hole and v_{rel}

is the relative velocity between the gas density and the black hole. This model can explain the relation of Rho, Cs and Mdot in the corner plot, however it can not explain the defference between the distribution of irresolvable black holes and resolvable black holes, which may help us understand the origin and formation of super massive black holes.

Table 3. Parameters description of the corner plot.

Parameters	Units	Description
Rho	-	Local gas density in the vicinity of the blackhole
Cs	-	Local gas sound-speed in the vicinity of the blackhole
Time	Second(logarithmic)	Time (scale-factor) for each entry
Mdot	$10^{10}M_{\odot}/0.978Gyr$	The mass accretion rate onto the black hole, instantaneous
Mass	$M_{\odot}(logarithmic)$	Mass of one black hole in a merger pair
Redshift	Dimensionless	-
MrdSNR	Dimensionless	SNR(LISA) of merger events in the Merger-Ringdown phase
InspSNR	Dimensionless	SNR(LISA) of merger events in the Inspiral phase
Mass ratio	-	The ratio of the mass of two black holes in a merger pair
Total mass	$M_{\odot}(logarithmic)$	The total mass of two black holes in a merger pair
Dl	Parsecs	Luminosity distance

4. Discussion and conclusions

This paper provides a new method to study the assembly of SMBHs in our universe. However, we emphasize that our model is phenomenological and that there are a number of caveats that may affect our results.

IllustrisTNG is based on the black holes seeding of $10^6 M_{\odot}$. Therefore it cannot show the different result of different seeding simulation. For example, for different BH seeds, redshift distribution, detecting ability and event rates of those GW detectors could be different, which may be able to help us understand the first SMBHs formation of the early universe.Furthermore, IllustrisTNG has limited resolution. It cannot resolve many BH parameters such as the spin parameter, which may affect the calculation of Gravitational waves. Overall, with these caveats in mind, a strong result from our calculations is that the third generation space-based GW detectors will be able to detect SMBHs in the mass range of $\sim 10^6 - 10^8\ M_{\odot}$ in the redshift range up to $z \sim 6$.

To summarize, we have calculated GW signals from SMBH mergers of a mass range $\sim 10^6 - 10^9\ M_{\odot}$ at redshifts $z \sim 0 - 6$, by post-processing the merger trees extracted from IllustrisTNG(TNG100) with a phenomenological GW model. Numerous super massive black hole mergers may occur, and these merger events may be detectable by space-based GW detectors such as LISA, Tianqin and Taiji. Space-based detectors can detect SMBHs of a wider mass range. LISA, Tianqin and Taiji will be able to detect both BBH inspirals and mergers of $\sim 10^6 - 10^7 M_{\odot}$ with an estimated event rate of 1 events per year at redshifts up to $z \sim 6$. While BBO and DECIGO may not be able to detect any super massive black hole merger event. The result of event rates in this study is in good consistency with the results in similar

study[5] whose events for LISA is about two mergers of both Merger-Ringdown and Inspiral phase per year. There are some interesting parameters distribution discrepencies between resolvable SMBH mergers and irrsolvable mergers. For example, the distribution difference in local gas density may lead to the distribution difference in the mass accretion rate, which could provide some evidence on the formation of the super massive black holes. We found out that the distribution of the local gas density in the vicinity of the blackhole has two peaks, but LISA can only detect one peak from the distribution. Besides, there are also two peaks in the distribution of the mass accretion rate of total BHs, although one peak is very low and flat. Together with the distribution of Mdot and Rho, there are 3 peaks for all the supermassive black holes in the simulation, as shown in the corner plot. However, only one peak out of three can be detected, which may shed light on the mechanism of the formation of super massive black holes in the early universe.

These results demonstrate that GW detectors will be powerful tools to study SMBHs in the Universe, which will be promising to probe different BH seed models and unravel the origin of the SMBHs.

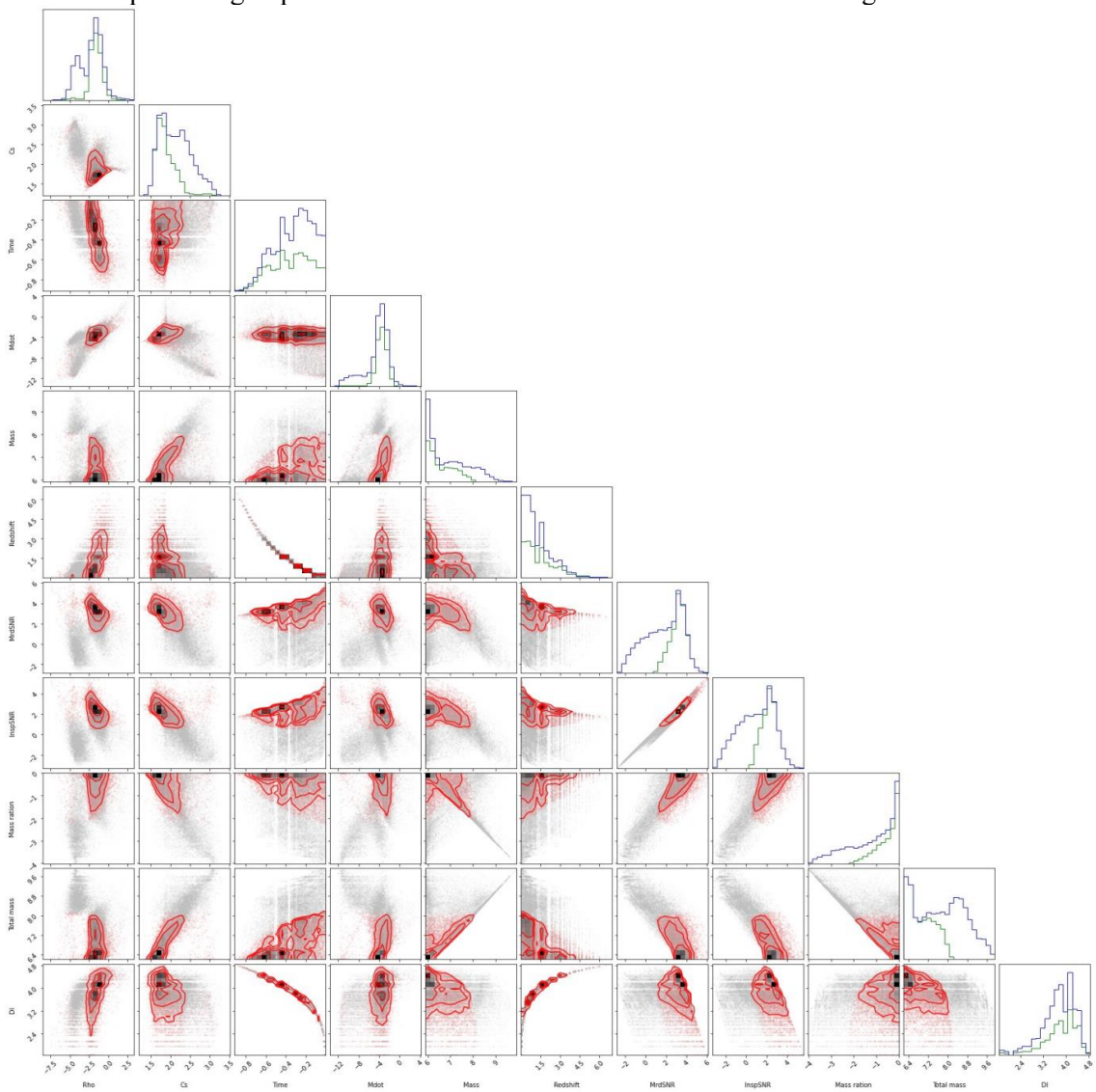

Figure 2. Corner plot of several parameters and distributions these parameters of the SMBH coalescence events from IllustrisTNG (detected by LISA). The histograms in green show the parameters distributions of irresolvable merger events while the histograms in blue show the parameters distributions of resolvable merger events. The description of the parameters can be seen in table 3.

Acknowledgments
We thank Dr. Mark Hannam for providing the code of the PhenomD model for gravitational waves calculations. We thank the IllustrisTNG collaboration for sharing simulation data which constituted the analysis in the large part of this paper.

References
[1] Buonanno A and Sathyaprakash BS 2014 *Preprint* arXiv:1410.7832
[2] Amaro-Seoane P, Audley H, Babak S, Baker J, Barausse E, Bender P, Berti E, Binetruy P, Born M, Bortoluzzi D and Camp J *Preprint* arXiv:1702.00786
[3] Colpi M, Holley-Bockelmann K, Bogdanovic T, Natarajan P, Bellovary J, Sesana A, Tremmel M, Schnittman J, Comerford J, Barausse E and Berti E 2019 *Preprint* arXiv:1903.06867
[4] Haehnelt MG *Monthly Notices of the Royal Astronomical Society* 1994 **269** 199-208
[5] Salcido J, Bower RG, Theuns T, McAlpine S, Schaller M, Crain RA, Schaye J and Regan J. *Monthly Notices of the Royal Astronomical Society* 2016 **463** 870-85
[6] Nelson D, Springel V, Pillepich A, Rodriguez-Gomez V, Torrey P, Genel S, Vogelsberger M, Pakmor R, Marinacci F, Weinberger R and Kelley L *CompAC* 2019 **6** 1-29
[7] Blanchet L *Living Rev. Relativ.* 2014 17 1-87
[8] Buonanno A and Damour T *Phys. Rev. D* 1999 **59** 084006
[9] Vishveshwara CV *Nature* 1970 **227** 936-8
[10] Sathyaprakash BS and Dhurandhar SV *Phys. Rev. D* 1991 **44** 3819
[11] Finn LS and Thorne KS *Physical Review D* 2000 **62** 124021.
[12] Husa S, Khan S, Hannam M, Pürrer M, Ohme F, Forteza XJ and Bohé A *Physical Review D* 2016 **93** 044006
[13] Kumar P, Chu T, Fong H, Pfeiffer HP, Boyle M, Hemberger DA, Kidder LE, Scheel MA and Szilagyi B *Physical Review D* 2016 93 104050
[14] Barausse E, Matarrese S and Riotto A *Physical Review D* 2005 **71** 063537
[15] Moore CJ, Cole RH and Berry CP *Class Quantum Gravity* 2014 **32** 015014
[16] Mei J, Bai YZ, Bao J, Barausse E, Cai L, Canuto E, Cao B, Chen WM, Chen Y, Ding YW and Duan HZ *Prog. Theor. Phys.* 2021 **2021** 05A107
[17] Yagi K and Seto N *Physical Review D* 2011 **83** 044011
[18] Flanagan EE and Hughes SA *Physical Review D* 1998 **57** 4566
[19] Koushiappas SM and Zentner AR *Astrophys. J.* 2006 **639** 7